Direct Detection of Leptophobic Dark Matter with Electronic Collective Excitations*

Yuanlin Gong (龚远林)[1] Yifan Hu (胡一凡)[1] Ning Liu (刘宁)[1,2] Liangliang Su (苏亮亮)[3†] Bin Zhu (祝斌)[4]

[1]Department of Physics and Institute of Theoretical Physics, Nanjing Normal University, Nanjing, 210023, China
[2]Nanjing Key Laboratory of Particle Physics and Astrophysics, Nanjing, 210023, China
[3]Institute for Astroparticle Physics (IAP), Karlsruhe Institute of Technology (KIT), Hermann-von-Helmholtz-Platz 1, D-76344 Eggenstein-Leopoldshafen, Germany
[4]Department of Physics, Yantai University, Yantai 264005, China

Abstract: Some next-generation dark matter detection experiments are primarily designed to search for dark matter--electron interactions, but they can also be used to probe models in which dark matter couples exclusively to nucleons via quantum effects. Hadronic loop-induced interactions can directly excite plasmons in semiconductors, thereby providing an additional channel for detecting leptophobic dark matter. In this work, we investigate plasmon excitations in silicon detectors induced by boosted dark matter and cosmic-ray upscattered dark matter via the hadronic loop process. By analyzing available experimental data, we derive new exclusion limits on the leptophobic dark matter--nucleon scattering cross section in the sub-MeV mass range.

Keywords: Leptophobic dark matter, boosted dark matter, cosmic-ray upscattered dark matter, plasmon excitation, semiconductor detectors

DOI: 10.1088/1674-1137/aeb6d3 **CSTR:**

CPC Accepted

I. INTRODUCTION

A wealth of gravitational evidence from astrophysical and cosmological observations compellingly supports the existence of dark matter (DM), which constitutes the majority of the mass content of the Universe. Consequently, various detection experiments have been developed and numerous DM candidates have been proposed to better understand DM. However, the fundamental nature and composition of DM, particularly its non-gravitational interactions and mass, remain unknown. For instance, the most widely studied DM candidate, weakly interacting massive particles (WIMPs) [1] with masses ranging from $O(1)$ GeV to $O(10)$ TeV, has not yielded any conclusive signals in direct detection experiments [2–4]. Meanwhile, the DM community has increasingly focused on non-WIMP DM candidates, such as sub-GeV DM [5–28], and on the development of novel detector materials [29–42], including semiconductor-based detectors [43–51].

Conventional DM direct detection experiments typically target nuclear recoil signals, whereas semiconductor experiments focus on electronic excitation signals induced by DM-electron interactions, enabling searches for lighter DM candidates. For semiconductors, the DM-electron scattering rate can be described by the energy loss function (ELF) of the material, $\mathrm{Im}[-\epsilon^{-1}(\mathbf{Q},\omega)]$, which depends on the momentum- and frequency-dependent longitudinal dielectric function $\epsilon(\mathbf{Q},\omega)$. This quantity can be calculated using density functional theory, including many-body effects, as in Refs. [52–55]. The ELF exhibits a significant enhancement of the excitation rate in certain kinematic regions, such as $|\mathbf{Q}| < 5$ keV and $\omega \sim 15$ eV for silicon detectors, as shown in Ref. [53]. This phenomenon is known as electronic collective, or plasmon, excitation, and is a common feature of well-ordered solid materials. The plasmon excitation regions of some conventional and unconventional materials can be found in Ref. [56] and [57], respectively. Recently, Refs. [58–61] investigated the potential of direct plasmon excitations as probes of DM-electron scattering. In particular, Ref. [58] clearly demonstrated that direct plasmon excitation requires the kinematic condition $v_\chi \gtrsim 0.01c$, and further calculated the corresponding excitation rate induced by re-

Received 1 July 2026; Accepted 21 October 2026

* N. Liu is supported by the National Natural Science Foundation of China (NNSFC) under Grant Nos. 12275134 and 12335005. L. Su is supported by the Alexander von Humboldt Foundation. B. Zhu is supported by the National Natural Science Foundation of China (NNSFC) under Grant No. 12275232.

† E-mail: E-mail: liangliang.su@kit.edu

Content from this work may be used under the terms of the Creative Commons Attribution 3.0 licence. Any further distribution of this work must maintain attribution to the author(s) and the title of the work, journal citation and DOI. Article funded by SCOAP[3] and published under licence by Chinese Physical Society and the Institute of High Energy Physics of the Chinese Academy of Sciences and the Institute of Modern Physics of the Chinese Academy of Sciences and IOP Publishing Ltd

lativistic DM-electron interactions.

Previous studies of direct electronic collective excitations have primarily focused on DM-electron interactions, such as those mediated by a dark photon or within leptophilic DM frameworks. In contrast, for well-motivated scenarios in which DM couples only to nucleons, direct electronic signals cannot be generated at tree level. Nevertheless, such DM can directly produce observable electron signals through hadronic loop-induced interactions with electrons, thereby enabling the detection of lighter DM, as demonstrated in Ref. [62]. Motivated by this, in this work we investigate direct electronic collective excitations induced by leptophobic DM (LDM) [63–67] via a proton-loop process.

We first identify the kinematic requirements for direct plasmon excitation by LDM, which similarly demand an LDM speed greater than $0.01c$. As benchmark scenarios, we consider two relativistic LDM fluxes: two-component boosted DM (BDM) [68–74] and cosmic-ray upscattering DM (CRDM) [75–93]. We then recalculate the plasmon excitation rate from LDM-electron scattering mediated by hadronic loops and use data from the SENSEI experiment at SNOLAB [94] to estimate the corresponding detection sensitivity in the sub-MeV mass range. This analysis yields new exclusion limits on the spin-independent LDM-nucleon scattering cross section through a light vector mediator.

II. LEPTOPHOBIC DARK MATTER–ELECTRON SCATTERING IN SEMICONDUCTORS

When LDM particles reach semiconductor detectors, they cannot couple directly to electrons at tree level because the mediator is leptophobic. However, their interactions can arise indirectly through hadronic loops, as shown in Fig. 1. The Dirac fermion LDM χ interacts with Standard Model particles through a vector mediator V that couples only to quarks. The simplest model introduces the vector mediator as the gauge boson associated with a local $U(1)_B$ baryon-number symmetry broken at the TeV or electroweak scale, as shown in various UV completions [95–101]. Within an appropriate low-energy effective theory [63], the Lagrangian can be written as

$$\mathcal{L} \supset g_B V_\mu J_B^\mu + g_\chi V_\mu \bar{\chi}\gamma^\mu \chi, \tag{1}$$

where $J_B^\mu = \frac{1}{3}\sum_q \bar{q}\gamma^\mu q$ is the corresponding baryon current. The parameters g_χ and g_B denote the couplings of DM and quarks to the vector mediator, respectively. The relevant gauge anomalies can be canceled by additional fermions in the UV completion, which acquire masses through couplings to the spontaneous symmetry-breaking sector of $U(1)_B$. These fermions are typically sufficiently heavy to satisfy experimental bounds [102]. Depending on the gauge coupling, the gauge boson V can be as light as the eV scale [103–106]. In the energy regime considered here, the effective LDM-nucleon interaction Lagrangian is given by

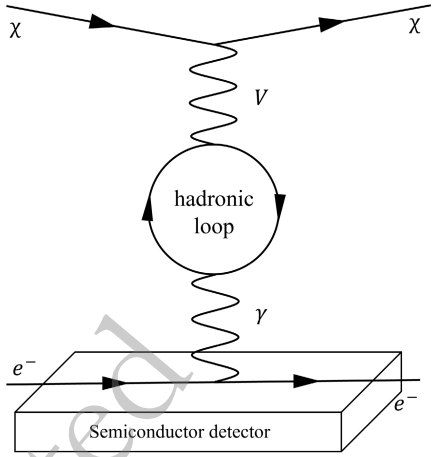


Fig. 1. Schematic diagram of the LDM–electron scattering process mediated by a hadronic loop in a semiconductor detector.

$$\langle N|g_B V_\mu J_B^\mu|N\rangle = g_B V_\mu \bar{N}\gamma^\mu N. \tag{2}$$

Proton or meson loops can induce mixing between the vector mediator and the photon, providing an effective coupling between LDM and electrons in a semiconductor detector, as shown in Fig 1. In this framework, the scattering amplitude $\mathcal{M}_{i\to f}$ for a bound-electron transition from the ground state $|i\rangle$ to a final state $|f\rangle$ with energy ω_f, induced by LDM-electron scattering, can be written as

$$\begin{aligned}\mathcal{M}_{i\to f} &= g_\chi \bar{u}_\chi(p'_\chi)\gamma^\mu u_\chi(p_\chi)\frac{g_{\mu\nu}}{m_V^2 - q^2}\frac{g_{\omega\xi}}{q^2} \\ &\times \Pi_{\nu\omega}^{\rm loop}\bar{u}_e(p'_e)\gamma^\xi u_e(p_e) \\ &= \bar{u}_\chi(p'_\chi)\gamma^0 u_\chi(p_\chi)\frac{e g_\chi}{m_V^2 - q^2}\left(\frac{c_{\rm loop}}{48\pi^2}\right) \\ &\times \langle f|\hat{\rho}(\mathbf{Q})|i\rangle 2\pi\delta(\omega_f - \omega),\end{aligned} \tag{3}$$

where m_V is the vector mediator mass, and the transferred four-momentum is represented as $q = (\omega, \mathbf{Q})$, with ω and $\mathbf{Q}$ denoting the transferred energy and three-momentum, respectively. The factor $\Pi_{\nu\omega}^{\rm loop}$ denotes the hadronic loop contribution, which is given by

$$\Pi_{\nu\omega}^{\rm loop} = \frac{e}{48\pi^2} g_{\nu\omega} q^2 c_{\rm loop}, \tag{4}$$

with

CPC Accepted

$$c_{\rm loop} = 4g_B \ln\left(\frac{4\pi e^{-\gamma_E}\Lambda^2}{m_p^2}\right), \tag{5}$$

Here, $m_p = 938$ MeV is the proton mass, and e is the elementary charge. In this work, we assume universal mediator couplings to quarks, such that the dominant hadronic loop contribution is generated exclusively by the proton loop. Consequently, contributions from the dominant light-meson loops, including pion and kaon loops, cancel identically (see Ref. [62] for details). Following the standard treatment in baryon chiral effective field theory (see, e.g., Ref. [107]), we take the ultraviolet cutoff to be of the order of the hadronic (or chiral symmetry-breaking) scale, $\Lambda \sim O(1\,\text{GeV})$, and choose $\Lambda = m_p$ as the benchmark value in our numerical calculations. We further set the Euler–Mascheroni constant to $\gamma_E = 0.577$.

In the second line of Eq. 3, only the timelike component is retained, since the spatial components are suppressed in the nonrelativistic bound-state regime of semiconductor electrons, as discussed in Ref. [58]. The electron density operator in momentum space, $\hat{\rho}(\mathbf{Q})$, is related to the energy loss function (ELF) of the semiconductor,

$$\text{Im}\left(-\frac{1}{\epsilon(\mathbf{Q},\omega)}\right) = \frac{\pi e^2}{Q^2}\sum_f |\langle f|\hat{\rho}(\mathbf{Q})|0\rangle|^2 \delta\left(\omega_f - \omega\right), \tag{6}$$

where $\epsilon(\mathbf{Q},\omega)$ is the material dielectric function, which is isotropic for the silicon detector, i.e., $\epsilon(\mathbf{Q},\omega) = \epsilon(Q,\omega)$. In this work, we adopt the ELF results from the *DarkELF* package [53].

Using the scattering amplitude, the transition rate of electronic excitation induced by LDM in the silicon detector can be obtained as

$$\begin{aligned}\Gamma\left(p_\chi\right) &= \sum_f \int \frac{\mathrm{d}^3 p'_\chi}{(2\pi)^3}\frac{\left|\mathcal{M}_{i\to f}\right|^2}{4E_\chi E'_\chi} 2\pi\delta\left(\omega + E'_\chi - E_\chi\right) \\ &= \int \frac{\mathrm{d}^3\mathbf{Q}}{(2\pi)^3}\left(\frac{(2E_\chi-\omega)^2 - Q^2}{4E_\chi(E_\chi-\omega)}\right) 2\frac{Q^2}{e^2} \\ &\times \text{Im}\left(-\frac{1}{\epsilon(Q,\omega)}\right)\left[\frac{e g_\chi c_{loop}}{48\pi^2(Q^2-\omega^2+m_V^2)}\right]^2 \\ &= \int \frac{\mathrm{d}^3\mathbf{Q}}{(2\pi)^3}\frac{\pi\bar{\sigma}_{\chi n}\left[(2E_\chi-\omega)^2 - Q^2\right]Q^2}{2\mu_{\chi n}^2 E_\chi(E_\chi-\omega)} \\ &\times \left(\frac{c_{\rm loop}}{48\pi^2 g_B}\right)^2 |F_{\rm DM}(q)|^2 \,\text{Im}\left(-\frac{1}{\epsilon(Q,\omega)}\right),\end{aligned} \tag{7}$$

where $E_\chi(E'_\chi)$ represents the energy of the initial (final) LDM particle, $\mu_{\chi n}$ is the DM–nucleon reduced mass, and the DM form factor in the last line is defined as

$$|F_{\rm DM}(q)|^2 = \begin{cases} 1 & \text{heavy med} \\ \left(\dfrac{\alpha m_e}{q}\right)^4 & \text{light med} \end{cases}, \tag{8}$$

where m_e is the electron mass and α is the fine-structure constant. In this work, we focus on the light-mediator case, $m_V^2 \ll q^2$, in which the DM form factor is enhanced at low momentum transfers in semiconductor detectors. We also define a momentum-independent LDM–nucleon cross section, $\bar{\sigma}_{\chi n} \equiv \dfrac{\mu_{\chi n}^2 g_\chi^2 g_B^2}{\pi(\alpha^2 m_e^2 + m_V^2)^2}$.

Given the differential flux of LDM, $\mathrm{d}\Phi_\chi/\mathrm{d}T_\chi$, the event rate for electronic excitations induced by LDM in semiconductors can be expressed as

$$\begin{aligned}\frac{\mathrm{d}R}{\mathrm{d}\omega} &= \int \frac{\mathrm{d}T_\chi}{\rho_T}\int \frac{\mathrm{d}\Omega}{4\pi}\frac{\mathrm{d}\Phi_\chi}{\mathrm{d}T_\chi}\frac{E_\chi}{|\vec{p}_\chi|}\Gamma\left(p_\chi\right)\delta\left(E'_\chi - E_\chi + \omega\right) \\ &= \frac{\bar{\sigma}_{\chi n}}{2\pi\rho_T}\frac{c_{\rm loop}^2}{(48\pi^2\mu_{\chi n} g_B)^2}\int Q^3\mathrm{d}Q\int_{E_\chi^{\rm min}}\mathrm{d}E_\chi\frac{\mathrm{d}\Phi_\chi}{\mathrm{d}T_\chi} \\ &\times \frac{(2E_\chi-\omega)^2 - Q^2}{4v_\chi^2 E_\chi^2}|F_{\rm DM}(q)|^2\,\text{Im}\left[\frac{-1}{\epsilon(Q,\omega)}\right],\end{aligned} \tag{9}$$

where ρ_T is the mass density of the target material in solid detectors. The parameter $E_\chi^{\rm min} = \sqrt{(|\vec{p}_\chi| - |\vec{q}|)^2 + m_\chi^2} + \omega$ denotes the minimum LDM energy required to excite an electron signal with energy ω.

However, direct plasmon excitation requires additional kinematic conditions. For example, in DM-electron scattering via a dark photon mediator, the DM velocity must exceed $0.01c$ [58]. For LDM-electron scattering via a hadronic loop, the vector mediator–photon mixing induced by the loop does not alter the four-momentum transfer before and after the loop, making the process analogous to the dark photon case. Consequently, the kinematic condition for direct plasmon excitation induced by LDM is the same as that in Ref. [58], namely, $v_\chi \gtrsim 0.01c$. In this work, we therefore consider two mechanisms capable of producing relativistic DM: boosted DM in a two-component DM model and cosmic-ray upscattering of DM (CRDM).

A. Boosted Dark Matter in a Two-Component Model

A commonly studied framework for relativistic DM is boosted DM in a two-component DM model. In this model, DM consists of two species, χ_1 and χ_2, with masses satisfying $m_{\chi_1} > m_{\chi_2}$. The lighter DM species, χ_2, can be as light as the eV scale, and its population may contribute to the radiation energy density in the early universe and modify the effective number of neutrino species during Big Bang Nucleosynthesis (BBN). However, the two-component DM species can decouple from the SM plasma around the QCD phase transition, resulting in a

CPC Accepted

dark-sector temperature T_D lower than the neutrino temperature T_ν because of the annihilation of degrees of freedom in the Standard Model (SM) plasma [108, 109]. Therefore, the contribution of the relativistic component χ_2 to the change in the effective number of neutrino species, $\Delta N_{\rm eff}$, during BBN is suppressed by $(T_D/T_\nu)^4$ and is compatible with current constraints [108]. The heavier DM species, χ_1, which constitutes the dominant DM component, does not couple directly to SM particles and achieves the correct relic abundance through annihilation into the lighter DM species, $\chi_1\bar{\chi}_1 \to \chi_2\bar{\chi}_2$. The mass hierarchy between the two species imparts a Lorentz boost to χ_2, with $\gamma_m = m_{\chi_1}/m_{\chi_2}$. Thus, the lighter DM species χ_2 is often referred to as boosted dark matter (BDM), which can be relativistic depending on the mass splitting $\Delta m_\chi = m_{\chi_1} - m_{\chi_2}$. In this work, the BDM χ_2 interacts with SM particles through the Lagrangian in Eq. 1.

The differential flux of BDM χ_2 from the Galactic center (GC) can then be calculated by

$$\frac{{\rm d}\Phi_{\rm BDM}}{{\rm d}E_{\chi_2}} = \frac{1}{4\pi}\frac{\langle\sigma v\rangle}{4m_{\chi_1}^2} J(\Omega) 2\delta(E_{\chi_2} - m_{\chi_1}) \tag{10}$$

where $\langle\sigma v\rangle$ denotes the thermally averaged annihilation cross section for $\chi_1\bar{\chi}_1 \to \chi_2\bar{\chi}_2$, and the term $2\delta(E_{\chi_2} - m_{\chi_1})$ indicates that the annihilation process produces two monoenergetic BDM particles, χ_2. The astrophysical $J(\Omega)$ factor is defined as the three-dimensional integral of the DM density over the target solid angle on the sky,

$$J(\Omega) = \int {\rm d}\Omega \int_{\rm l.o.s} \rho_\chi^2(r(x,\theta)){\rm d}x, \tag{11}$$

where $\rho_\chi(r)$ denotes the DM density profile, and the Galactocentric distance is given by $r = \sqrt{d_\odot^2 + x^2 - 2xd_\odot\cos\theta}$. Here, x is the line-of-sight (l.o.s.) distance from the Earth, $d_\odot = 8.127$ kpc is the distance from the Sun to the GC, and θ is the angle between the Earth-GC axis and the l.o.s.

In this work, we adopt the Navarro-Frenk-White (NFW) DM density profile and follow the results of Ref. [68]. The all-sky flux of BDM is given by

$$\frac{{\rm d}\Phi_{\rm BDM}}{{\rm d}E_{\chi_2}} = 4.0\times10^{-7}{\rm cm}^{-2}{\rm s}^{-1}\left(\frac{\langle\sigma v\rangle}{5\times10^{-26}\ {\rm cm}^3{\rm s}^{-1}}\right) \times\left(\frac{20\ {\rm GeV}}{m_{\chi_1}}\right)^2 \delta(E_{\chi_2} - m_{\chi_1}). \tag{12}$$

B. Cosmic-Ray Upscattered Dark Matter

In addition to BDM in two-component DM models, another widely studied relativistic component of the DM flux arises from cosmic-ray upscattered DM, commonly referred to as CRDM. In this framework, DM in the Milky Way halo can be accelerated through scattering with high-energy cosmic rays.

Accordingly, the differential flux of CRDM can be written as

$$\begin{aligned}\frac{{\rm d}\Phi_{\rm CRDM}}{{\rm d}T_\chi} &= \int \frac{{\rm d}\Omega}{4\pi}\int_{\rm l.o.s}^{\infty}{\rm d}s\int_{T_p^{min}}^{\infty}{\rm d}T_p\frac{\rho_\chi}{m_\chi}\frac{{\rm d}\sigma_{\chi n}}{{\rm d}T_\chi}\frac{{\rm d}\Phi_p}{{\rm d}T_p}\\ &= D\frac{\rho_0}{m_\chi}\int_{T_p^{\rm min}}^{\infty}{\rm d}T_p\frac{{\rm d}\sigma_{\chi n}}{{\rm d}T_\chi}\frac{{\rm d}\Phi_p^{\rm LIS}}{{\rm d}T_p},\end{aligned} \tag{13}$$

with the differential cross section for DM–proton elastic scattering evaluated in the rest frame of the DM particles,

$$\begin{aligned}\frac{{\rm d}\sigma_{\chi n}}{{\rm d}T_\chi} = \frac{\bar{\sigma}_{\chi n}|F_{\rm DM}(q)|^2F_p^2(q^2)}{4\mu_{\chi p}^2(2m_pT_p + T_p^2)}[2m_\chi(T_p+m_p)^2\\ + m_\chi T_\chi^2 - 2m_\chi T_pT_\chi - T_\chi(m_p+m_\chi)^2],\end{aligned} \tag{14}$$

where T_p and T_χ are the kinetic energies of the CR proton and the DM particle, respectively. For light nuclei such as the proton, the nucleon form factor is often parameterized by the dipole form

$$F_p(q^2) = \frac{1}{(1+q^2/\Lambda_p^2)^2}, \tag{15}$$

where $\Lambda_p \simeq 770$ MeV is associated with the proton charge radius. The minimum kinetic energy of the proton is

$$T_p^{\rm min} = \left(\frac{T_\chi}{2} - m_p\right)\left[1 \pm \sqrt{1 + \frac{2T_\chi}{m_\chi}\frac{(m_p+m_\chi)^2}{(2m_p - T_\chi)^2}}\right], \tag{16}$$

where the + (−) sign corresponds to $T_\chi > 2m_p$ ($T_\chi < 2m_p$). For $T_\chi = 2m_p$, the minimal kinetic energy is given by $\sqrt{m_p/m_\chi}\,(m_p + m_\chi)$.

In this work, we consider only the contribution from the local interstellar (LIS) proton spectrum, which can be parameterized as ${\rm d}\Phi_p^{\rm LIS}/{\rm d}T_p = 4\pi({\rm d}R_p/{\rm d}T_p)({\rm d}I_p/{\rm d}R_p)$, where R_p denotes the CR proton rigidity [110]. The contribution from DM–electron scattering is suppressed by the proton loop and can therefore be neglected. We also assume a homogeneous CR distribution and define the effective distance as $D \equiv \frac{1}{4\pi\rho_0}\int_{\rm l.o.s}\rho_\chi\,{\rm d}s\,{\rm d}\Omega$, which evaluates to $D = 8.02$ kpc under the assumption of an NFW DM profile with local density $\rho_0 = 0.4\ {\rm GeV/cm}^3$ and a l.o.s. integration up to 10 kpc [75]. An inhomogeneous CR distribution over a larger volume would result in a larger effective distance and thus a higher CRDM flux [77, 111]; however, this is beyond the scope of this work.

CPC Accepted

III. RESULTS

To more clearly illustrate the electronic excitation induced by BDM and CRDM in a silicon detector, the top panel of Fig. 2 shows the differential event rate $\mathrm{d}R/\mathrm{d}\omega$ for 1 keV BDM (solid line: $m_{\chi_1} = 1\,\mathrm{MeV}$, $m_{\chi_2} = 1\,\mathrm{keV}$) and CRDM (dashed line), assuming a DM–nucleon scattering cross section of $\bar{\sigma}_{\chi n} = 10^{-32}\,\mathrm{cm}^2$. The event rates exhibit a pronounced enhancement in the region $10\,\mathrm{eV} < \omega < 25\,\mathrm{eV}$ for both BDM and CRDM. This enhancement is consistent with the plasmon excitation region shown in Fig. 1 of Ref. [58] and with observations from electron energy loss spectroscopy [112].

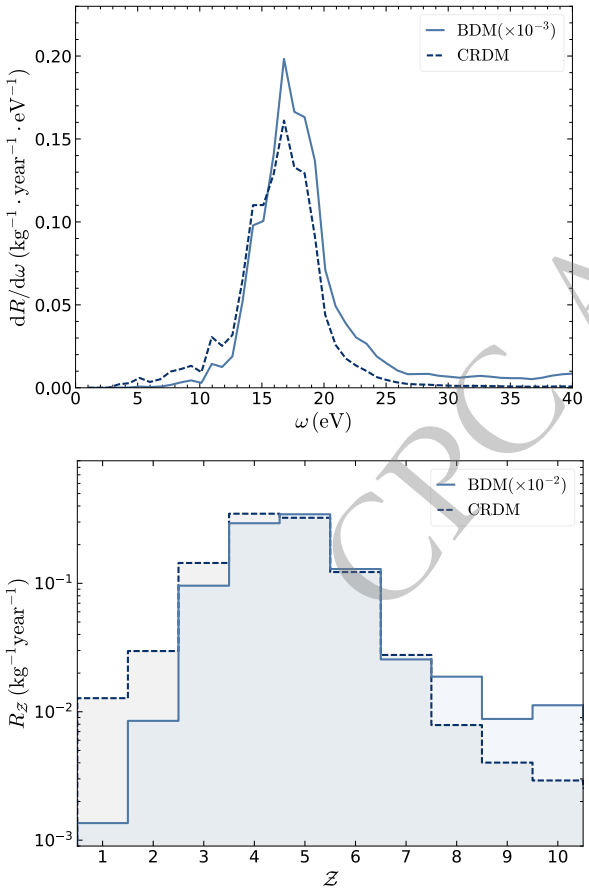


Fig. 2. *Top panel:* Differential event rate $\mathrm{d}R/\mathrm{d}\omega$ as a function of the deposited energy ω; *Bottom panel:* Event rate $R_{\mathcal{Z}}$ as a function of the ionization charge $\mathcal{Z}$. The solid lines denote the BDM case with $m_{\chi_1} = 1$ MeV, $m_{\chi_2} = 1$ keV, and a thermally averaged annihilation cross section of $\langle\sigma v\rangle = 5\times 10^{-26}\,\mathrm{cm}^3/\mathrm{s}$. The dashed lines show the results for 1 keV CRDM. The benchmark DM–nucleon scattering cross section is $\bar{\sigma}_{\chi n} = 10^{-32}\,\mathrm{cm}^2$.

For semiconductor detectors such as the SENSEI and DAMIC-M experiments, the electronic excitation signal is observed through secondary electron-hole pairs, and its relationship with the differential event rate is as follows:

$$R_{\mathcal{Z}} = \int \mathrm{d}\omega P(\mathcal{Z}|\omega)\frac{\mathrm{d}R}{\mathrm{d}\omega}, \tag{17}$$

where $\mathcal{Z}$ denotes the ionization charge corresponding to secondary electron–hole pairs. The function $P(\mathcal{Z}|\omega)$ denotes the pair-creation probability distribution, which represents the probability of producing $\mathcal{Z}$ ionization pairs for a given deposited energy ω. Moreover, this probability depends on temperature. In this work, we use the results for $P(\mathcal{Z}|\omega)$ at 100 K from Ref. [113], which is close to the operating temperatures of the SENSEI and DAMIC-M experiments. The corresponding band gap energy and mean energy per pair are $E_{\mathrm{gap}} = 1.16$ eV and $\epsilon = 3.75$ eV, respectively. Thus, for the study of plasmon excitation, we focus on deposited energies ω ranging from E_{gap} to 50 eV. The bottom panel of Fig. 2 shows the event rate $R_{\mathcal{Z}}$ as a function of the ionization charge $\mathcal{Z}$. The plasmon excitations induced by BDM and CRDM via a hadronic loop are found to lie in the range of 3–6 electron–hole pairs.

The SENSEI experiment has recently reported multi-electron results, observing four $3e^-$ events and zero events in the 4–6e^- range, with an unmasked-pixel exposure of 100.72 gram·days [94]. The corresponding 90% confidence level (C.L.) upper limits on the number of events and the effective exposures are summarized in Table I. Furthermore, the DAMIC-M experiment has reported one $4e^-$ event with an exposure of 1.3 kg·days [50], which is consistent with the results of the SENSEI experiment. However, we do not present the corresponding constraints from the DAMIC-M experiment in this work because of the lack of effective exposure information.

Table 1. The 90% C.L. upper limits on the number of observed events in the 3–6e^- range are taken from the SENSEI experiment [94].

Ionized Charge $\mathcal{Z}$	Exposures (gram·days)	Event Number
$3e^-$	57.71	8.6
$4e^-$	63.03	2.3
$5e^-$	65.56	2.3
$6e^-$	67.31	2.3

By combining the experimental results with the theoretical event rate in Eq. 17, we derive the 90% C.L. exclusion limits by requiring that the predicted number of events not exceed the observed limits. For the BDM scenario in the two-component model, we first present the exclusion limits from each of the 3–6e^- bins in the $\bar{\sigma}_{\chi n}$-Δm_χ plane, as shown in Fig. 3, to investigate the impact of the boost factor of BDM χ_2. In the top panel, the mass of the heavier component is fixed at $m_{\chi_1} = 1\,\mathrm{MeV}$, while the lighter component mass m_{χ_2} is varied from the keV to the

CPC Accepted

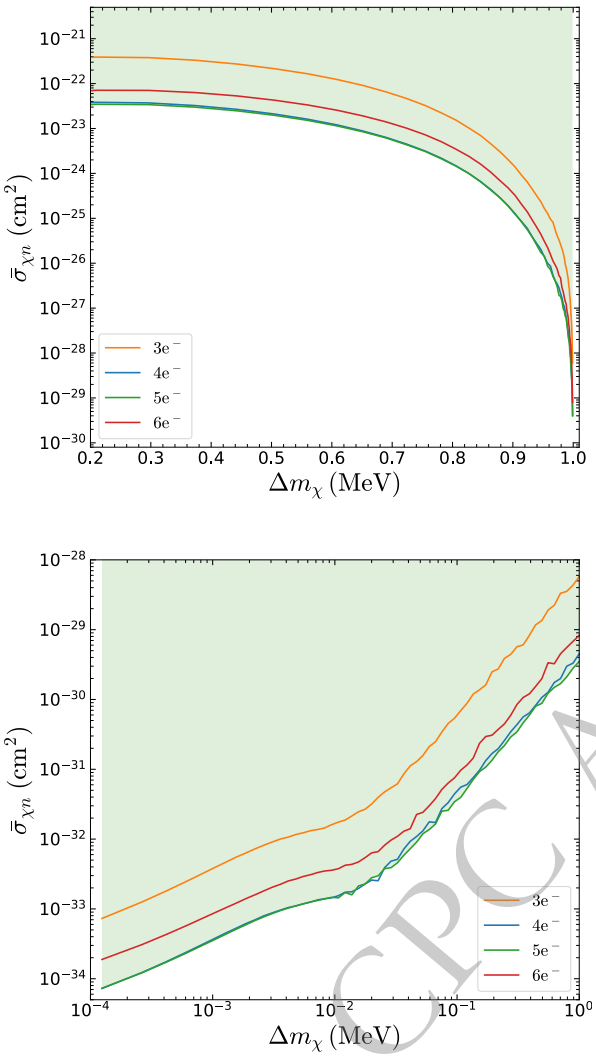


Fig. 3. The 90% confidence-level exclusion limits on the LDM–nucleon scattering cross section $\bar{\sigma}_{\chi n}$ are shown as functions of the mass splitting $\Delta m_\chi = m_{\chi_1} - m_{\chi_2}$ in the two-component BDM model. *Top panel:* results for a fixed heavier-component mass of $m_{\chi_1} = 1$ MeV. *Bottom panel:* results for a fixed lighter-component mass of $m_{\chi_2} = 1$ keV.

MeV scale. We find that the constraints become weaker as Δm_χ decreases, corresponding to a larger m_{χ_2}. This behavior arises because the electronic excitation rate in Eq. 9 scales approximately with the inverse square of the reduced mass, $R \propto 1/\mu_{\chi n}^2 \sim 1/m_{\chi_2}^2$. By contrast, in the bottom panel, the lighter component is fixed at $m_{\chi_2} = 1$ keV, and the mass of the heavier component is varied. The mass of the heavier component affects the electronic excitation rate not only through the BDM flux (Eq. 12) but also via the factor $S = \dfrac{(2E_\chi - \omega)^2 - Q^2}{4v_\chi^2 E_\chi^2}$ in Eq. 9. For $\Delta m_\chi \gg m_{\chi_2}$, the factor S remains approximately constant. However, as Δm_χ or m_{χ_1} decreases, the factor S becomes suppressed by m_{χ_1}, leading to a change in the slope of the exclusion limits around $\Delta m_\chi \sim 20$ keV. This trend ceases once the mass splitting becomes too small to produce (semi-)relativistic BDM, i.e., $v_\chi \gtrsim 10^{-2}c$. Moreover, the results in Fig. 3 indicate that the strongest constraint arises from the $5e^-$ observation in the SENSEI experiment. Therefore, in the following discussion, we focus on the constraint from the $5e^-$ bin.

In Fig. 4, we present the 90% C.L. constraints on the LDM-nucleon cross section $\bar{\sigma}_{\chi n}$ as a function of the DM mass m_χ (or m_{χ_2}) for both the BDM and CRDM scenarios. For the two-component BDM case, we consider two benchmark values for the heavier component, $m_{\chi_1} = 1$ MeV (dashed blue line) and $m_{\chi_1} = 0.1$ MeV (solid blue line), motivated by the results in Fig. 3. As shown in the figure, smaller values of m_{χ_1} lead to more stringent constraints on the BDM-nucleon scattering cross section, consistent with the trend observed in the bottom panel of Fig. 3. The exclusion limit from CRDM-induced plasmon excitation (red line) is similar to that obtained for the two-component BDM scenario with $m_{\chi_1} = 1$ MeV. Several cosmological and astrophysical constraints are also shown in this parameter space, including those from the CMB measured by Planck 2015 [114, 115] (purple), Milky Way satellite galaxies [116] (green), and the Lyman-α forest [117] (yellow). A large DM-nucleon cross section can suppress the DM flux reaching the detector through interactions with the Earth, thereby reducing the experimental sensitivity. A typical reference value for this cross section is $O(10^{-28})$ cm^2 [118, 119]. Our results

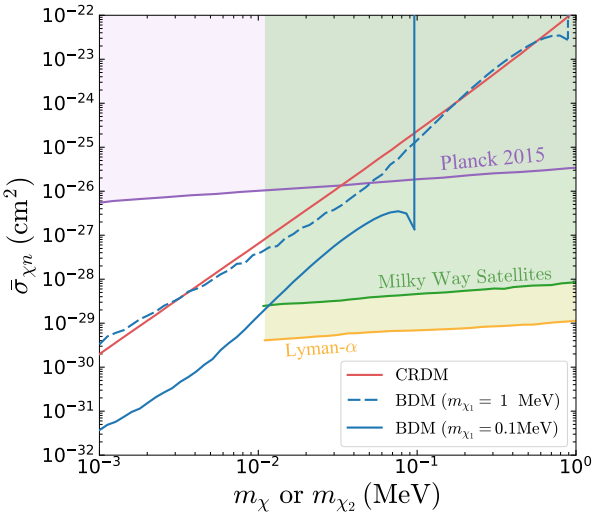


Fig. 4. The 90% C.L. upper limits on the LDM–nucleon scattering cross section $\bar{\sigma}_{\chi n}$ are shown as a function of the DM mass. The red line corresponds to CRDM, whereas the dashed and solid blue lines represent the two-component BDM scenario with $m_{\chi_1} = 1$ MeV and $m_{\chi_1} = 0.1$ MeV, respectively. For comparison, existing cosmological and astrophysical constraints are also shown: CMB constraints from *Planck* 2015 [114, 115] (purple), Milky Way satellite galaxies [116] (green), and the Lyman-α forest [117] (yellow).

CPC Accepted

provide new exclusion limits on the LDM-nucleon scattering cross section based on the observation of electronic collective excitation. Finally, the light mediator V is subject to constraints from fifth-force searches [120], neutron scattering and neutron-optics experiments [121], and other probes [122, 123]. For the light-mediator mass range $m_V \ll 1\,\mathrm{keV}$ considered here, laboratory experiments constrain the gauge coupling to $g_B < 10^{-9}$ at $m_V \sim 20\,\mathrm{eV}$ [123]. In our work, for $m_{\chi_2} = 1\,\mathrm{keV}$ and $g_\chi = 1$, the BDM limits on g_B are $g_B < 2.5\times10^{-6}$ and 2.5×10^{-7} for $m_{\chi_1} = 1$ and $0.1\,\mathrm{MeV}$, respectively. For CRDM with $m_\chi = 1\,\mathrm{keV}$, the corresponding limit is $g_B < 1.8\times10^{-6}$.

IV. CONCLUSIONS

In this work, we investigated a class of leptophobic dark matter models in which tree-level DM-electron interactions are absent, whereas hadronic loop effects can effectively induce DM-electron scattering. These loop-induced interactions allow leptophobic dark matter to produce electronic excitation signals in dark matter detectors, particularly collective excitations (plasmons) in semiconductors. Such signals, in turn, provide constraints on the DM-nucleon scattering cross section through electronic signal measurements. To demonstrate the potential reach of this mechanism, we considered two representative relativistic dark matter scenarios: boosted dark matter in a two-component model and cosmic-ray upscattered dark matter. Both models naturally yield dark matter with velocities sufficiently high to excite plasmons in semiconductor targets. Using currently available experimental data, we derived new 90% confidence-level exclusion limits on the spin-independent DM-nucleon cross section for dark matter masses ranging from the keV to MeV scales. Our study shows that electronic collective excitations can serve as a powerful probe of leptophobic dark matter, extending the sensitivity of direct detection beyond the capabilities of conventional nuclear-recoil-based searches. Future detectors with lower thresholds and larger exposures will further enhance this potential, opening new opportunities to explore sub-GeV leptophobic dark matter through electronic signals.

CPC Accepted

References

[1] B. W. Lee and S. Weinberg, Phys. Rev. Lett. **39**, 165 (1977)
[2] Z. Bo, *et al*., Phys. Rev. Lett. **134**(1), 011805 (2025)
[3] J. Aalbers, *et al*., Phys. Rev. Lett. **135**(1), 011802 (2025)
[4] E. Aprile *et al*. (XENON), arXiv:2502.18005
[5] R. Essig, J. Mardon, and T. Volansky, Phys. Rev. D **85**, 076007 (2012)
[6] Y. Hochberg, Y. Zhao, and K. M. Zurek, Phys. Rev. Lett. **116**(1), 011301 (2016)
[7] Y. Hochberg, T. Lin, and K. M. Zurek, Phys. Rev. D **94**(1), 015019 (2016)
[8] S. Derenzo, R. Essig, A. Massari, *et al*., Phys. Rev. D **96**(1), 016026 (2017)
[9] M. Ibe, W. Nakano, Y. Shoji, *et al*., JHEP **03**, 194 (2018)
[10] M. J. Dolan, F. Kahlhoefer, and C. McCabe, Phys. Rev. Lett. **121**(10), 101801 (2018)
[11] S. Knapen, T. Lin, and K. M. Zurek, Phys. Rev. D **96**(11), 115021 (2017)
[12] R. Essig, J. Pradler, M. Sholapurkar, *et al*., Phys. Rev. Lett. **124**(2), 021801 (2020)
[13] V. V. Flambaum, L. Su, L. Wu, *et al*., Sci. China Phys. Mech. Astron. **66**(7), 271011 (2023)
[14] G. Elor, R. McGehee, and A. Pierce, Phys. Rev. Lett. **130**(3), 031803 (2023)
[15] L. Su, L. Wu, and B. Zhu, Phys. Rev. D **105**(5), 055021 (2022)
[16] R. Calabrese, M. Chianese, D. F. G. Fiorillo, *et al*., Phys. Rev. D **105**(10), 103024 (2022)
[17] Z.-L. Liang, C. Mo, F. Zheng, *et al*., Phys. Rev. D, **106** (4): 043004 (2022), [Erratum: Phys.Rev.D 106, 109901 (2022)]
[18] J. Li, L. Su, L. Wu, *et al*., JCAP **04**, 020 (2023)
[19] Y. Gu, L. Wu, and B. Zhu, Phys. Rev. D **106**(7), 075004 (2022)
[20] L. Su, L. Wu, N. Zhou, *et al*., Phys. Rev. D **108**(3), 035004 (2023)
[21] S. Li, *et al*., Phys. Rev. Lett. **130**(26), 261001 (2023)
[22] J.-H. Liang, Y. Liao, X.-D. Ma, *et al*., Phys. Rev. D **110**(9), L091701 (2024)
[23] S. Balan, *et al*., JCAP **01**, 053 (2025)
[24] P. N. Bhattiprolu, R. McGehee, E. Petrosky, *et al*., Phys. Rev. D **111**(3), 035027 (2025)
[25] F. Lin, N. Liu, L. Su, *et al*., arXiv:2504.13007
[26] S. M. Griffin, G. D. Hadas, Y. Hochberg, *et al*., Phys. Rev. Lett. **135**(14), 141803 (2025)
[27] A. Cheek, P. Figueroa, G. Herrera, *et al*., arXiv:2507.15956
[28] L. Li, C.-T. Lu, A. K. Mishra, *et al*., arXiv:2509.11906
[29] P. W. Graham, D. E. Kaplan, S. Rajendran, *et al*., Phys. Dark Univ. **1**, 32 (2012)
[30] R. Essig, M. Fernandez-Serra, J. Mardon, *et al*., JHEP **05**, 046 (2016)
[31] Y. Hochberg, T. Lin, and K. M. Zurek, Phys. Rev. D **95**(2), 023013 (2017)
[32] S. Knapen, T. Lin, M. Pyle, *et al*., Phys. Lett. B **785**, 386 (2018)
[33] N. A. Kurinsky, T. C. Yu, Y. Hochberg, *et al*., Phys. Rev. D **99**(12), 123005 (2019)
[34] T. Trickle, Z. Zhang, and K. M. Zurek, Phys. Rev. Lett. **124**(20), 201801 (2020)
[35] A. Coskuner, A. Mitridate, A. Olivares, *et al*., Phys. Rev. D **103**(1), 016006 (2021)
[36] R. M. Geilhufe, F. Kahlhoefer, and M. W. Winkler, Phys. Rev. D **101**(5), 055005 (2020)
[37] S. M. Griffin, Y. Hochberg, K. Inzani, *et al*., Phys. Rev. D **103**(7), 075002 (2021)

[38] E. Andersson, A. Bökmark, R. Catena, *et al.*, JCAP **05**, 036 (2020)
[39] A. Esposito and S. Pavaskar, Phys. Rev. D **108**(1), L011901 (2023)
[40] S. Autti, *et al.*, Eur. Phys. J. C **84**(3), 248 (2024)
[41] F. Toschi, *et al.*, Phys. Rev. D **111**(3), 032013 (2025)
[42] L. Baudis *et al.* (QROCODILE), arXiv:2412.16279
[43] A. Aguilar-Arevalo, *et al.*, Phys. Rev. D **94**(8), 082006 (2016)
[44] L. Barak, *et al.*, Phys. Rev. Lett. **125**(17), 171802 (2020)
[45] Q. Arnaud, *et al.*, Phys. Rev. Lett. **125**(14), 141301 (2020)
[46] D. W. Amaral, *et al.*, Phys. Rev. D **102**(9), 091101 (2020)
[47] A. Aguilar-Arevalo *et al.* (Oscura), arXiv:2202.10518
[48] Z. Y. Zhang, *et al.*, Phys. Rev. Lett. **129**(22), 221301 (2022)
[49] I. M. Bloch, *et al.*, Phys. Rev. Lett. **134**(16), 161002 (2025)
[50] K. Aggarwal, *et al.*, Phys. Rev. Lett. **135**(7), 071002 (2025)
[51] P. Abbamonte *et al.*, arXiv:2507.17782
[52] S. Knapen, J. Kozaczuk, and T. Lin, Phys. Rev. D **104**(1), 015031 (2021)
[53] S. Knapen, J. Kozaczuk, and T. Lin, Phys. Rev. D **105**(1), 015014 (2022)
[54] C. Boyd, Y. Hochberg, Y. Kahn, *et al.*, Phys. Rev. D **108**(1), 015015 (2023)
[55] C. E. Dreyer, R. Essig, M. Fernandez-Serra, *et al.*, Phys. Rev. D **109**(11), 115008 (2024)
[56] N. Kurinsky, D. Baxter, Y. Kahn, *et al.*, Phys. Rev. D **102**(1), 015017 (2020)
[57] Y. Hochberg, D. Novko, R. Ovadia, *et al.*, arXiv:2507.07164
[58] Z.-L. Liang, L. Su, L. Wu, *et al.*, Phys. Rev. Lett. **134**(7), 071001 (2025)
[59] R. Essig, R. Plestid, and A. Singal, Commun. Phys. **7**(1), 416 (2024)
[60] J.-W. Sun, L. Wu, Y.-H. Xu, *et al.*, arXiv:2501.07591
[61] J. B. Dent, B. A. Friedman, J. L. Newstead, *et al.*, arXiv:2510.06574
[62] M. Diamond, C. V. Cappiello, A. C. Vincent, *et al.*, Phys. Rev. Lett. **132**(5), 051001 (2024)
[63] B. Batell, P. deNiverville, D. McKeen, *et al.*, Phys. Rev. D **90**(11), 115014 (2014)
[64] P. Coloma, B. A. Dobrescu, C. Frugiuele, *et al.*, JHEP **04**, 047 (2016)
[65] J. A. Dror, R. Lasenby, and M. Pospelov, Phys. Rev. Lett. **119**(14), 141803 (2017)
[66] A. Berlin, N. Blinov, G. Krnjaic, *et al.*, Phys. Rev. D **99**(7), 075001 (2019)
[67] A. Boyarsky, O. Mikulenko, M. Ovchynnikov, *et al.*, JHEP **03**, 006 (2022)
[68] K. Agashe, Y. Cui, L. Necib, *et al.*, JCAP **10**, 062 (2014)
[69] B. Fornal, P. Sandick, J. Shu, *et al.*, Phys. Rev. Lett. **125**(16), 161804 (2020)
[70] D. Borah, M. Dutta, S. Mahapatra, *et al.*, Phys. Lett. B **820**, 136577 (2021)
[71] A. Basu, A. Chakraborty, N. Kumar, *et al.*, Phys. Rev. D **111**(9), 095016 (2025)
[72] J. Li, T. Nomura, J. Pei, *et al.*, Phys. Rev. D **108**(3), 035021 (2023)
[73] K. Choi and J.-C. Park, arXiv:2409.05646
[74] H. Alhazmi, D. Kim, K. Kong, *et al.*, arXiv:2503.13598
[75] T. Bringmann and M. Pospelov, Phys. Rev. Lett. **122**(17), 171801 (2019)
[76] Y. Ema, F. Sala, and R. Sato, Phys. Rev. Lett. **122**(18), 181802 (2019)
[77] C. V. Cappiello and J. F. Beacom, Phys. Rev. D, **100** (10): 103011 (2019), [Erratum: Phys.Rev.D 104, 069901 (2021)]
[78] W. Wang, L. Wu, J. M. Yang, *et al.*, JHEP, **12**: 072 (2020), [Erratum: JHEP 02, 052 (2021)]
[79] S.-F. Ge, J. Liu, Q. Yuan, *et al.*, Phys. Rev. Lett. **126**(9), 091804 (2021)
[80] C. Xia, Y.-H. Xu, and Y.-F. Zhou, Nucl. Phys. B **969**, 115470 (2021)
[81] Y. Ema, F. Sala, and R. Sato, SciPost Phys. **10**(3), 072 (2021)
[82] N. F. Bell, J. B. Dent, B. Dutta, *et al.*, Phys. Rev. D **104**, 076020 (2021)
[83] W. Wang, L. Wu, W.-N. Yang, *et al.*, Phys. Rev. D **107**(7), 073002 (2023)
[84] X. Cui, *et al.*, Phys. Rev. Lett. **128**(17), 171801 (2022)
[85] T. N. Maity and R. Laha, Eur. Phys. J. C **84**(2), 117 (2024)
[86] K. I. Nagao, S. Higashino, T. Naka, *et al.*, JCAP **07**, 061 (2023)
[87] N. F. Bell, J. L. Newstead, and I. Shaukat-Ali, Phys. Rev. D **109**(6), 063034 (2024)
[88] L. Su, L. Wu, and B. Zhu, Sci. China Phys. Mech. Astron. **67**(2), 221012 (2024)
[89] X. Shang, *et al.*, Phys. Rev. Lett. **133**(10), 101805 (2024)
[90] T. Herbermann, M. Lindner, and M. Sen, Phys. Rev. D **110**(12), 123023 (2024)
[91] R. Diurba and H. Kolešová, JHEP **07**, 202 (2025)
[92] R. A. Gustafson, G. Herrera, M. Mukhopadhyay, *et al.*, arXiv:2508.20984
[93] Z. Chen, S.-F. Ge, J. Li, *et al.*, arXiv:2509.12007
[94] P. Adari, *et al.*, Phys. Rev. Lett. **134**(1), 011804 (2025)
[95] A. E. Nelson and N. Tetradis, Phys. Lett. B **221**, 80 (1989)
[96] S. Rajpoot, Phys. Rev. D **40**, 2421 (1989)
[97] R. Foot, G. C. Joshi, and H. Lew, Phys. Rev. D **40**, 2487 (1989)
[98] X.-G. He and S. Rajpoot, Phys. Rev. D **41**, 1636 (1990)
[99] P. Fileviez Perez and M. B. Wise, JHEP **08**, 068 (2011)
[100] M. Duerr, P. Fileviez Perez, and M. B. Wise, Phys. Rev. Lett. **110**, 231801 (2013)
[101] P. Fileviez Perez and S. Ohmer, Phys. Lett. B **768**, 86 (2017)
[102] B. A. Dobrescu and C. Frugiuele, Phys. Rev. Lett. **113**, 061801 (2014)
[103] P. Fayet, Class. Quant. Grav. **13**, A19 (1996)
[104] P. Fayet, Phys. Rev. D **75**, 115017 (2007)
[105] V. V. Nesvizhevsky, G. Pignol, and K. V. Protasov, Phys. Rev. D **77**, 034020 (2008)
[106] Z. Bogorad, P. W. Graham, and G. Gratta, Phys. Rev. D **108**(5), 055005 (2023)
[107] T. Becher and H. Leutwyler, Eur. Phys. J. **9**(4), 643 (1999)
[108] J. F. Cherry, M. T. Frandsen, and I. M. Shoemaker, Phys. Rev. Lett. **114**, 231303 (2015)
[109] D. McKeen and N. Raj, Phys. Rev. D **99**(10), 103003 (2019)
[110] M. J. Boschini, *et al.*, Astrophys. J. **840**(2), 115 (2017)
[111] C. Xia, Y.-H. Xu, and Y.-F. Zhou, Phys. Rev. D **107**(5),

CPC Accepted

055012 (2023)
[112] M. K. Kundmann, *Study of semiconductor valence plasmon line shapes via electron energy-loss spectroscopy in the transmission electron microscope*, Ph.D. thesis, Lawrence Berkeley National Laboratory, California (1988)
[113] K. Ramanathan and N. Kurinsky, Phys. Rev. D **102**(6), 063026 (2020)
[114] N. Aghanim, *et al*., Astron. Astrophys. **594**, A11 (2016)
[115] V. Gluscevic and K. K. Boddy, Phys. Rev. Lett. **121**(8), 081301 (2018)
[116] E. O. Nadler, V. Gluscevic, K. K. Boddy, *et al*., Astrophys. J. Lett., **878** (2): 32 (2019), [Erratum: Astrophys.J.Lett. 897, L46 (2020), Erratum: Astrophys.J. 897, L46 (2020)]
[117] K. K. Rogers, C. Dvorkin, and H. V. Peiris, Phys. Rev. Lett. **128**(17), 171301 (2022)
[118] C. Xia, Y.-H. Xu, and Y.-F. Zhou, JCAP **02**(02), 028 (2022)
[119] N. Kumar and G. Lekshmi, Phys. Rev. D **111**(5), 055022 (2025)
[120] J. Murata and S. Tanaka, Class. Quant. Grav. **32**(3), 033001 (2015)
[121] H. Leeb and J. Schmiedmayer, Phys. Rev. Lett. **68**, 1472 (1992)
[122] E. Rrapaj and S. Reddy, Phys. Rev. C **94**(4), 045805 (2016)
[123] J. M. Berryman, S. Gardner, and M. Zakeri, Symmetry **14**(3), 518 (2022)

CPC Accepted